Synthesis, Structures, and Redox Properties of Copper Complexes with Chiral and Achiral Amino Acid Derived Ligands

Nicole Niklas,[a] Frank Hampel,[b] Olaf Walter,[c] Günter Liehr,[a] and Ralf Alsfasser*[a]

Keywords: Amino acids / Chirality / Copper / Redox chemistry

A series of copper(II) complexes containing the amino acid derived ligands bpaAc-Gly-OEt {**1**; [bis(picolyl)amino]acylglycine ethyl ester} and bpaAc-Phe-OMe {**2**; [bis(picolyl)amino]acylphenylalanine methyl ester} were synthesized and characterized in solution and in the solid state. This was done in order to evaluate the relevance of weak aromatic interactions between a metal center and amino acid side chains in square-pyramidal or octahedral coordination environments. The results showed that the structural, spectroscopic, and electrochemical properties of the copper(II) center are not affected by the amino acid side chain structure. This is in remarkable contrast to our previous investigations on zinc(II) complexes of the same ligands, which indicate close association of the metal center and the phenyl substituent of **2** in a trigonal-bipyramidal environment.

Introduction

Aromatic rings are important structural and functional elements both in biological and in synthetic supramolecular architectures. They significantly contribute to the intramolecular stabilization of structures, as well as to the formation of intermolecular complexes.[1–6] This is achieved either through noncovalent ring stacking[7] or through π-cation interactions.[8,9] Furthermore, the redox-active aromatic amino acids tyrosine and tryptophan are known to participate in metalloenzyme-catalyzed substrate oxidations.[10]

The quest for synthetic metalloenzyme mimetics has stimulated much interest in the characterization of weak aromatic ring/cation interactions in small coordination complexes.[11–16] We have recently reported trigonal-bipyramidal zinc complexes of the amino acid derived ligands bpaAc-Gly-OEt (**1**) and bpaAc-Phe-OMe (**2**), shown in Scheme 1 {bpaAc = [bis(2-picolyl)amino]acyl; Gly-OEt = glycine ethyl ester; Phe-OMe = phenylalanine methyl ester}.[17] Intriguing features of the phenylalanine derivatives are: (i) the relatively short distance of 4.5 Å between the zinc ion and the center of the phenyl ring, and (ii) a rigid conformation of the benzyl side chain in solution. The latter is evidenced by analysis of the proton NMR chemical shifts and coupling constants.

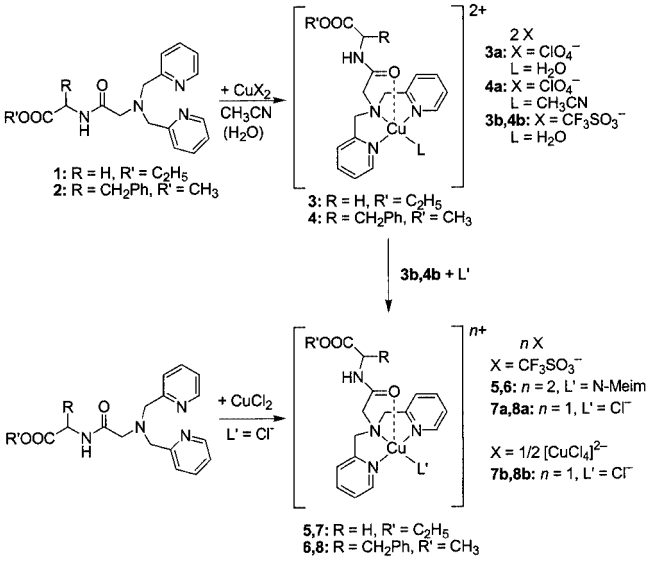

Scheme 1. Copper(II) coordination chemistry of bpaAc-Gly-OEt (**1**) and bpaAc-Phe-OMe (**2**)

Here we report the synthesis and characterization of copper(II) complexes containing **1** and **2**. This was done in order to evaluate specific geometric requirements for the occurrence of weak aromatic interactions in complexes containing our tripodal N_3O ligand framework. In contrast to our findings for trigonal-bipyramidal zinc complexes, X-ray structure analyses together with electrochemical, EPR, and

[a] Institute of Inorganic Chemistry, University of Erlangen-Nürnberg,
Egerlandstr. 1, 91058 Erlangen, Germany
Fax: (internat.) + 49-(0)9131/852-7387
E-mail: alsfasser@chemie.uni-erlangen.de
[b] Institute of Organic Chemistry, University of Erlangen-Nürnberg,
Henkestrasse 42, 91054 Erlangen, Germany
[c] ITC-CPV, Forschungszentrum Karlsruhe,
Postfach 3640, 76021 Karlsruhe

circular dichroism measurements in solution demonstrated that the phenyl ring in **2** is flexible in square-pyramidal copper(II) compounds and does not efficiently interact with the metal center.

Results

Synthesis

All reactions are summarized in Scheme 1. The complexes [(bpaAc-Gly-OEt)(H_2O)Cu](ClO_4)$_2$ (**3a**), [(bpaAc-Gly-OEt)(H_2O)Cu](OTf)$_2$ (**3b**, OTf = CF_3SO_3), [(bpaAc-Phe-OMe)(CH_3CN)Cu](ClO_4)$_2$ (**4a**), and [(bpaAc-Phe-OMe)(H_2O)Cu](OTf)$_2$ (**4b**) were readily obtained from acetonitrile solutions containing stoichiometric amounts of the respective ligand and copper(II) salt. The *N*-methylimidazole complex [(bpaAc-Gly-OEt)(*N*-Meim)Cu](OTf)$_2$ (**5**) was similarly formed in one-pot reaction mixtures containing stoichiometric amounts of the ligand **1**, *N*-Meim, and Cu(OTf)$_2$. This was not the case for the sterically more demanding ligand **2**, with only [(*N*-Meim)$_5$Cu](OTf)$_2$ and bpaAc-Phe-OMe being isolated under the same conditions. However, the complex [(bpaAc-Phe-OMe)(*N*-Meim)Cu](OTf)$_2$ (**6**) was readily obtained by substitution of the labile aquo ligand from **4b**. This method worked equally well in the synthesis of **5** from **3b**.

Ligand exchange from **3b** and **4b** was also a convenient route to generate the chloro complexes [(bpaAc-Gly-OEt)Cu(Cl)](OTf) (**7a**) and [(bpaAc-Phe-OMe)Cu(Cl)](OTf) (**8a**) in situ for spectroscopic studies in solution. As we have reported earlier for the glycine derivative **7b**,[18] the cations [LCuCl]$^+$ may also be synthesized by treatment of the respective ligand with copper(II) chloride. This method always results in the formation of chlorocuprate anions, which severely complicate spectroscopic investigations. However, the tetrachlorocuprate salt [(bpaAc-Phe-OMe)Cu(Cl)]$_2$[$CuCl_4$] (**8b**) was the only copper(II) complex of ligand **2**, other than the acetonitrile diperchlorate derivative **4a**, to yield single crystals suitable for an X-ray structure determination.

Structures

We have characterized the glycine derivatives **3a**, **3b**, and **5**, as well as the phenylalanine derivatives **4a** and **8b**, by X-ray structure analyses. ORTEP plots of the cations containing **1** are shown in Figures 1−3, and the cations containing **2** are presented in Figures 4 and 5. Crystallographic details are summarized in Table 1; the structure of **7b** has been reported elsewhere.[18] All complexes show a similar first coordination sphere with a typical Jahn−Teller-distorted octahedral geometry around the copper(II) center. The three bpa nitrogen atoms of the tripodal ligands are bound in the equatorial plane and the amide oxygen atom occupies one of the axial positions. The equatorial plane is completed by the respective monodentate coligand − water (**3a**, **3b**), CH_3CN (**4a**), *N*-Meim (**5**), or chloride (**8b**) − and a weakly coordinating anion (Cu−L > 2.5 Å) is located at the respective second axial sites in the complexes **3a**, **3b**, **4a**, and **5**. Pairs of cations are formed by **8b**, with the coordinated chloro ligand of one complex above the copper center of the other at a nonbonding distance of ca. 3.1 Å. Bond lengths and angles are compared in Table 2. The first coordination spheres within our series are very similar, and all structural parameters agree well with those of the closely related complexes described by Nishida et al.[19,20]

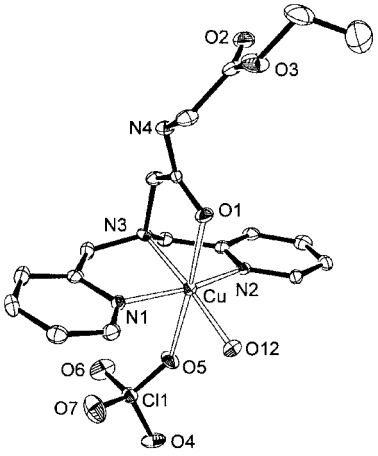

Figure 1. ORTEP plot (30% ellipsoids) of the cation [(bpaAc-Gly-OEt)(H_2O)Cu(ClO_4)]$^+$ (**3a**); hydrogen atoms are omitted for clarity

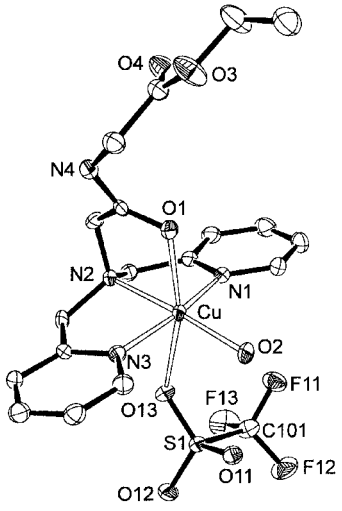

Figure 2. ORTEP plot (30% ellipsoids) of the cation [(bpaAc-Gly-OEt)(H_2O)Cu(CF_3SO_3)]$^+$ (**3b**); hydrogen atoms are omitted for clarity

Interesting are the different orientations adopted by the benzyl substituents in **4a** and **8b**. In both cases the structures are disordered. They refined best by assumption of two overlapping conformers with their phenyl rings in different orientations with respect to the equatorial plane defined by the first coordination sphere, as illustrated in Figures 4 and 5. The shortest distance between the copper(II) center and the phenyl ring center is observed in conformer B of **8b** (Figure 5; 7.24 Å). As a consequence of the disordered benzyl substituents and the disordered solvent mole-

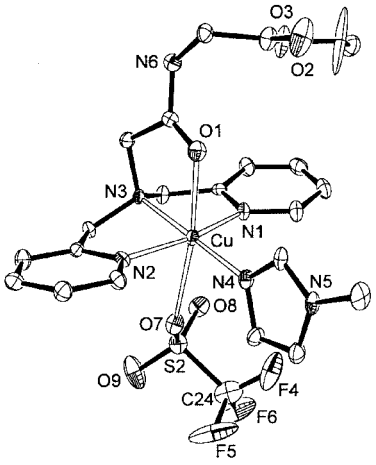

Figure 3. ORTEP plot (30% ellipsoids) of the cation [(bpaAc-Gly-OEt)(*N*-Meim)Cu(CF_3SO_3)]$^+$ (**5**); hydrogen atoms are omitted for clarity

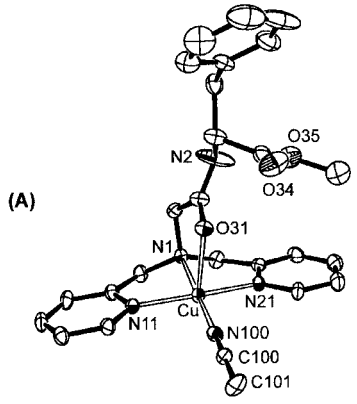

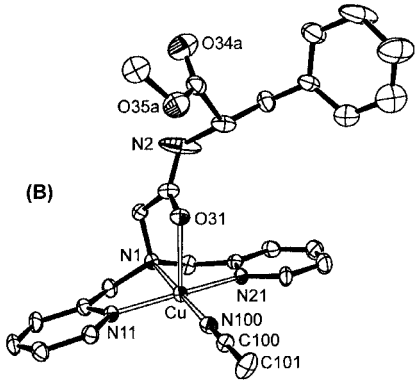

Figure 4. ORTEP plots (30% ellipsoids) of the two conformational isomers (A) and (B) of the cation [(bpaAc-Phe-OMe)(CH_3CN)Cu]$^{2+}$ (**4a**); hydrogen atoms have been omitted for clarity

cules in the asymmetric units (**4a**: CH_3CN; **8b**: 3 MeOH), both structures are of relatively poor quality. However, their similarity is striking and the data agree with the spectroscopic and electrochemical data reported below.

UV/Vis, EPR, and CD Spectroscopy

The UV/Vis spectra of our complexes in methanol were characterized by a weak metal-centered d-d band. Comparison showed that substitution of ligand **2** for ligand **1** did not significantly affect either λ_{max} or extinction coefficients. Differences were observed only between the various monodentate coligands. The spectra of the perchlorate and triflate salts **3a/3b** and **4a/4b** were very similar ($\lambda_{max} \approx 709$ nm, lg $\varepsilon \approx 1.86$), consistent with identical first coordination spheres around the copper(II) center. We therefore assume that the acetonitrile ligand in **4a** is rapidly exchanged in solution. This may also be true for the aquo ligands in **3a**, **3b**, and **4b**. With respect to the spectra of **3a**, **3b**, **4a**, and **4b**, the bands of the imidazole complexes were blue-shifted (**5**: $\lambda_{max} = 675$ nm, lg $\varepsilon = 1.93$; **6**: $\lambda_{max} = 681$ nm, lg $\varepsilon = 1.91$). The bands of the chloro complexes **7a** and **8a** appeared at longer wavelengths (**7a**: $\lambda_{max} = 725$ nm, lg $\varepsilon = 1.97$; **8a**: $\lambda_{max} = 732$ nm, lg $\varepsilon = 1.96$). Even larger red shifts and extinction coefficients were observed for the chlorocuprate salts **7b** and **8b** (**7b**: $\lambda_{max} = 757$ nm, lg $\varepsilon = 2.32$; **8b**: $\lambda_{max} = 755$, lg $\varepsilon = 2.30$). This behavior must be due to the anions, since the first coordination spheres are similar to those in **7a** and **8a**. Figure 6 illustrates the trend observed for the chloro complexes. Shown are the spectra of the aquo complexes **3b** and **4b**, their water/chloride exchange products **7a** and **8a**, and the chlorocuprate salts **7b** and **8b**.

The EPR spectra of our complexes were typical for copper(II) complexes with a $d_{x^2-y^2}$ ground state. All data obtained in frozen methanol solutions are summarized in Table 3. They confirmed that only the monodentate ligand had an effect on the *g* values and coupling constants,

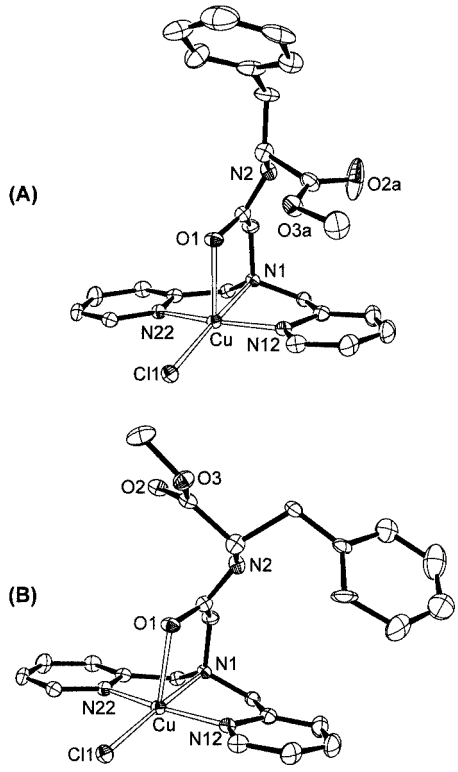

Figure 5. ORTEP plots (30% ellipsoids) of the two conformational isomers (A) and (B) of the cation [(bpaAc-Phe-OMe)Cu(Cl)]$^+$ (**8b**); hydrogen atoms have been omitted for clarity.

Table 1. Details of the X-ray structure analyses

Compound	**3a**·H_2O	**3b**·0.3CH_2Cl_2	**4a**·CH_3CN	**5**	**8b**·3CH_3OH
Empirical formula	$C_{18}H_{26}Cl_2CuN_4O_{13}$	$C_{20.3}H_{21}Cl_{0.6}CuF_6N_4O_{10}S_2$	$C_{28}H_{32}Cl_2CuN_6O_{11}$	$C_{24}H_{28}CuF_6N_6O_9S_2$	$C_{51}H_{91}Cl_6Cu_3N_8O_9$
Formula mass	640.87	743.94	763.04	786.18	1363.64
Temperature [K]	200(2)	200(2)	173(2)	200(2)	173(2)
Wavelength [Å]	0.71073	0.71073	0.71073	0.71073	0.71073
Crystal system	monoclinic	monoclinic	triclinic	monoclinic	triclinic
Space group	$P2_1/c$	$C2/c$	$P\bar{1}$	$P2_1/n$	$P\bar{1}$
a [Å]	16.82(5)	25.699(2)	7.8668(2)	8.49(5)	13.388(3)
b [Å]	9.37(5)	15.252(1)	9.2765(3)	25.95(5)	13.830(3)
c [Å]	16.23(5)	16.999(1)	24.0570(8)	14.77(5)	18.731(4)
α [°]	90	90	87.950(2)	90	89.10(3)
β [°]	95.1(2)	113.72	87.854(2)	91.3(2)	74.95(3)
γ [°]	90	90	78.381(2)	90	63.01(3)
Volume [Å^3]	2549(17)	6100.1(7)	1695.86(9)	3255(23)	2961.3(10)
Z	4	8	2	4	2
Calculated density [Mg/m^3]	1.670	1.620	1.494	1.604	1.529
Absorption coefficient [mm^{-1}]	1.139	0.998	0.867	0.892	1.398
F(000)	1316	3008	786	1604	1428
Crystal size [mm]	0.40 × 0.28 × 0.18	0.25 × 0.07 × 0.07	0.35 × 0.10 × 0.03	0.70 × 0.43 × 0.18	0.30 × 0.30 × 0.10
θ-range [°]	2.51−23.94	1.59−28.28	2.24−25.03	2.52−23.81	1.13−27.54
Index ranges	$0 \le h \le 19$	$-34 \le h \le 34$	$-9 \le h \le 9$	$0 \le h \le 9$	$-15 \le h \le 17$
	$-10 \le k = 10$	$-19 \le k \le 18$	$-11 \le k \le 11$	$-28 \le k \le 29$	$-17 \le k \le 17$
	$-18 \le l \le 18$	$-22 \le l \le 20$	$-28 \le l \le 28$	$-16 \le l \le 16$	$-24 \le l \le 24$
Reflections collected/unique	7989/4000	32657/7457	10690/5890	9832/4926	23590/13549
Refinement method	Based on F^2	Based on F^2	Based on F^2	Based on F^2	Based on F^2
Data/restraints/parameters	4000/38/343	7457/0/423	5890/34/470	4926/48/437	13549/0/893
Goodness-of-fit on F^2	1.064	1.039	1.129	1.179	1.226
Final R indices [$I > 2\sigma(I)$]	$R1 = 0.0605$	$R1 = 0.0599$	$R1 = 0.0870$	$R1 = 0.0598$	$R1 = 0.1022$
	$wR2 = 0.1509$	$wR2 = 0.1721$	$wR2 = 0.2277$	$wR2 = 0.1544$	$wR2 = 0.2583$
R indices (all data)	$R1 = 0.1146$	$R1 = 0.1281$	$R1 = 0.1128$	$R1 = 0.1096$	$R1 = 0.1253$
	$wR2 = 0.1939$	$wR2 = 0.2020$	$wR2 = 0.2402$	$wR2 = 0.1977$	$wR2 = 0.2710$
Largest diff. peak/hole [eÅ^{-3}]	1.123/−0.796	1.377/−0.796	0.828/−0.687	1.054/−0.662	1.750/−0.888

Table 2. Selected bond lengths [Å] and angles [°] with standard deviations given in parentheses

	3a	**3b**	**4a**	**5**	**8b**
$Cu-N^{am}$ [a]	2.037(11)	2.057(4)	2.048(6)	2.069(12)	2.067(6)
$Cu-N^{py}$ [b]	1.981(11)	1.981(4)	1.986(6)	2.017(12)	1.979(7)
	1.997(11)	1.992(4)	1.988(6)	2.030(12)	1.983(7)
$Cu-O^{ad}$ [c]	2.228(12)	2.278(3)	2.232(5)	2.326(14)	2.334(6)
$Cu-L^{eq}$ [d]	1.972(11)	1.985(3)	1.976(6)	1.990(12)	2.232(2)
$N^{am}-Cu-N^{py}$	83.7(2)	83.4(2)	83.2(2)	82.4(2)	83.3(3)
	82.2(2)	83.4 (2)	83.1(2)	82.4(2)	82.8(3)
$N^{am}-Cu-O^{ad}$	82.7(2)	81.9(1)	82.5(2)	81.4(2)	80.4(2)
$N^{am}-Cu-L^{eq}$	175.0(2)	176.2(2)	177.8(3)	179.4(2)	176.6(2)
$N^{py}-Cu-O^{ad}$	96.7(2)	96.0(2)	100.8(2)	90.7(2)	99.5(3)
	87.7(2)	89.6(1)	86.7(2)	91.8(2)	84.1(3)
$N^{py}-Cu-N^{py}$	164.5(2)	164.8 (2)	163.3(2)	164.0(2)	164.9(3)
$N^{py}-Cu-L^{eq}$	98.1(2)	98.7(2)	97.6(2)	98.3(2)	96.7(2)
	95.4(2)	94.1(2)	96.5(2)	97.0(2)	96.8(2)
$O^{ad}-Cu-L^{eq}$	102.2(2)	101.1 (1)	95.4(2)	98.6(2)	102.9(2)

[a] N^{am} = amine nitrogen atom of the bpa ligand fragment. [b] N^{py} = pyridine nitrogen atom of the bpa ligand fragment. [c] O^{ad} = amide oxygen atom. [d] L^{eq} = equatorial ligand atom (monodentate coligand).

whereas changes in the amino acid structures did not register. The spectra of the *N*-methylimidazole complexes **5** and **6** and the chloro complexes **7a** and **8a** were rhombic, whereas axial patterns were found for the aquo and acetonitrile species **3a**, **3b**, **4a**, and **4b**. The spectra of **7b** and **8b** appeared to be rhombic but were not well resolved, due to complications arising from the presence of different chlorocuprate anions.[18] It was therefore not possible to determine an accurate value of g_y for these complex salts.

Circular dichroism spectra were collected for the chiral L-phenylalanine derivatives **4a**, **4b**, **6**, **8a**, and **8b**. The results are shown in Figure 7. In agreement with the similarity of the structures, there was no significant observed difference between the spectra of **4a**, **4b**, and **6**. They closely resembled

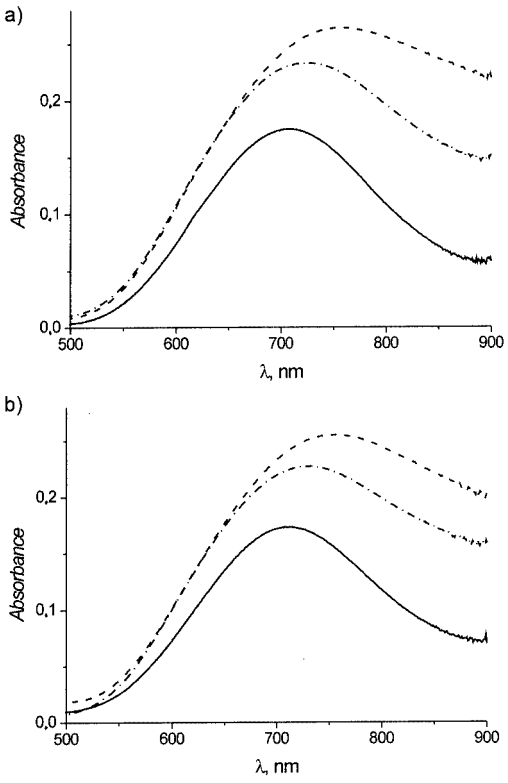

Figure 6. Vis spectra (0.002 M Cu^{2+} in methanol) of the triflate complexes **3b** (a) and **4b** (b) (——), the ligand exchange products **7a** (a) and **8a** (b) (–·–·), and the tetrachlorocuprate salts **7b** (a) and **8b** (b) (----)

Table 3. EPR spectra of the complexes in frozen methanol solutions (10^{-3} M Cu^{2+}; 120 K)

Compound	g_x	$g_\perp/g_y$	$g_\parallel/g_z$	$A_\parallel/A_z$ [10^{-4} cm^{-1}]
3a	–	2.06	2.27	170
3b	–	2.16	2.28	170
4a	–	2.05	2.26	169
4b	–	2.10	2.28	170
5	2.01	2.06	2.25	185
6	2.01	2.06	2.25	182
7a	1.94	2.03	2.23	170
7b	1.96	not resolved	2.25	175
8a	1.95	2.05	2.25	172
8b	1.96	not resolved	2.25	171

that of the free ligand **2**,[17] except for a 20 nm red shift of the pyridine ring π-π* transitions,[21] which appeared at 282 nm. In comparison, the corresponding free ligand signal is at 262 nm with a similar positive Cotton effect. Interestingly, the corresponding signal of $[(\mathbf{2})(H_2O)Zn](OTf)_2$ [17] exhibited a negative Cotton effect with a minimum at 270 nm. The chloro complexes **8a** and **8b** showed different behavior, exhibiting positive signals at ca. 289 nm significantly larger and broader than those of the other complexes studied. Though we cannot assign this band to a particular transition, it is interesting to note that the behavior is paralleled by a similar effect observed for the corresponding chlorozinc(II) complex.[22]

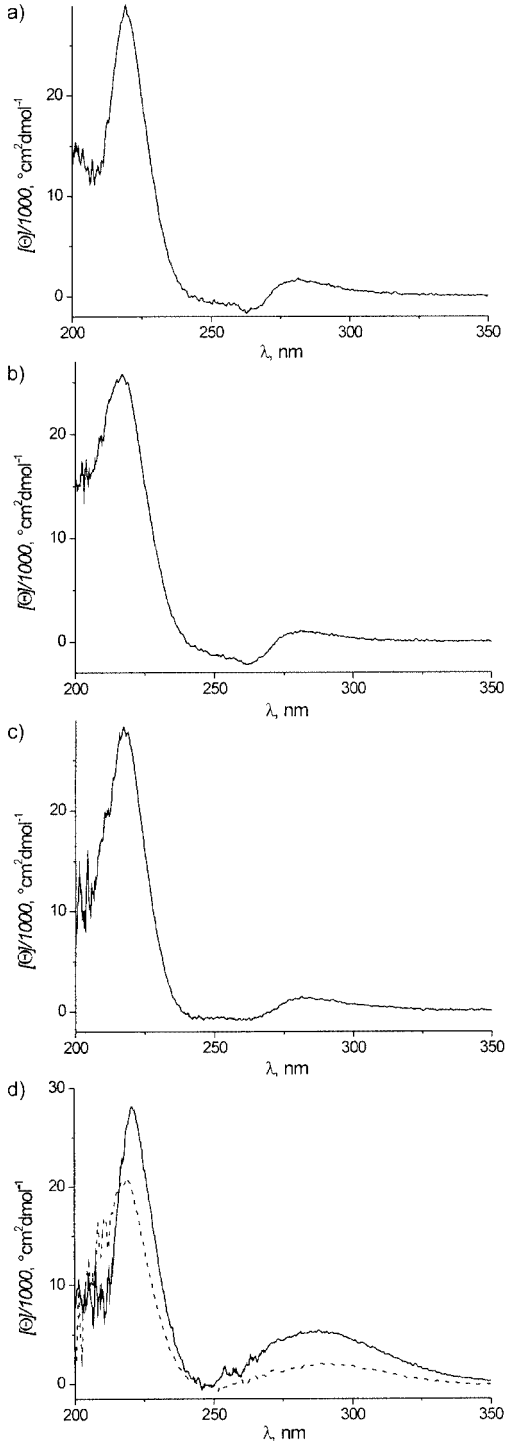

Figure 7. Circular dichroism spectra (0.001 M Cu^{2+} in methanol) of a) **4a**, b) **4b**, c) **6**, and d) **8a** (----) and **8b** (——)

Cyclic Voltammetry

The cyclic voltammograms of the complexes are shown in Figure 8 and the data are summarized in Table 4. In general, electrochemically quasireversible redox transitions were observed for all compounds. We assign these transitions to the Cu^{II}/Cu^{I} redox couple. The perchlorate and

triflate salts **3a/3b** and **4a/4b** exhibited broad shoulders at anodic potentials of ca. + 0.1 V. This feature is commonly encountered in copper(II) complexes and has been ascribed to adsorption processes at the glassy carbon working electrode.[23]

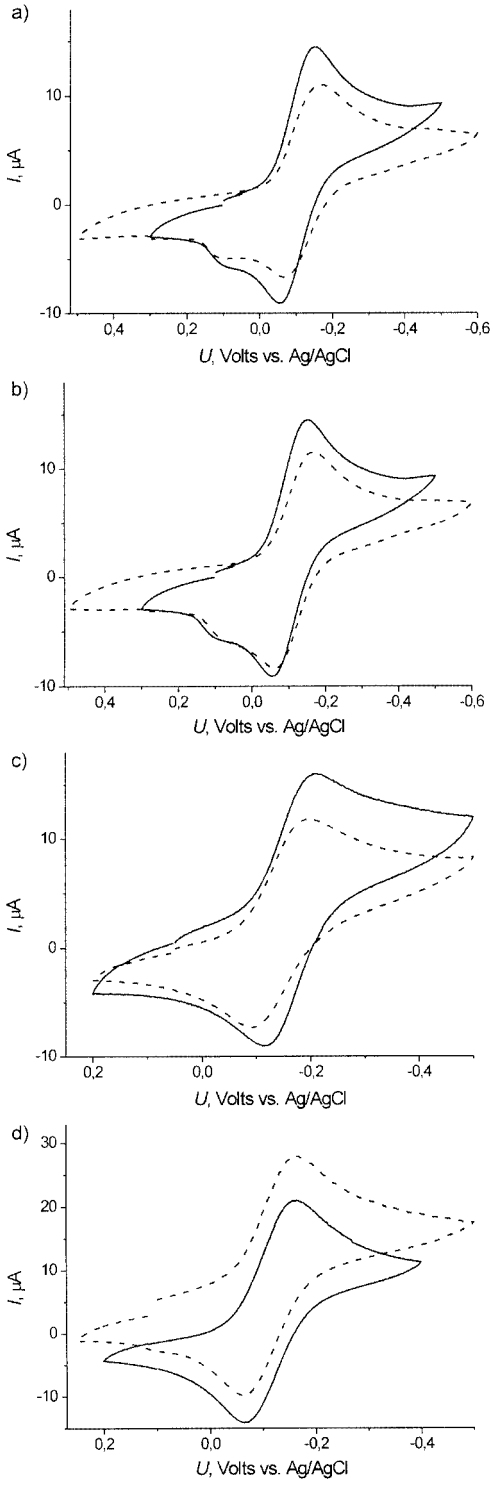

Figure 8. Cyclic voltammograms (0.1 M TBAH in methanol) of the complexes (10^{-3} M Cu^{2+}), a) **3a** and **4a**, b) **3b** and **4b**, c) **5** and **6**, d) **7b** and **8b** (——: bpaAc-Gly-OEt; ----: bpaAc-Phe-OMe)

Table 4. Electrochemical data ($E_{1/2}$ in V vs. Ag/AgCl; $\Delta E_{1/2}$ in mV) obtained for the complexes in 10^{-3} M methanol solutions at scan rates of 50 mV/s

Compd.	**3a**	**3b**	**4a**	**4b**	**5**	**6**	**7b**	**8b**
$E_{1/2}$	−0.10	−0.10	−0.10	−0.12	−0.16	−0.15	−0.11	−0.11
$\Delta E_{1/2}$	89	106	90	107	88	107	93	98

It is evident that no significant differences exist between complexes of the two ligands **1** and **2**. Considering the broad waves and the adsorption phenomena involved, the small shifts observed in $E_{1/2}$ for the triflate (**3a**, **4a**), perchlorate (**3b**, **4b**), and chloro (**7b**, **8b**) complexes are certainly well within the experimental errors. Small changes were only observed for the *N*-methylimidazole complexes **5** and **6**, which were reduced at potentials ca. −50 mV more negative than for the other compounds. In view of the accuracy of cyclic voltammetry, however, this shift may also not be significant.

Discussion

Our earlier investigations on zinc(II) complexes of ligand **2** demonstrated that a trigonal-bipyramidal coordination geometry resulted in an unusual conformational stability of the noncoordinating benzyl substituent.[17] We have now incorporated **2** in square-pyramidal copper(II) complexes. This was done in order to evaluate the effects of different geometries on the formation of noncovalent interactions between metal ions and aromatic amino acid side chains in tripodal ligand frameworks.

Both ligands **1** and **2** form copper complexes that are typical members of the tpa family [tpa: tris(picolyl)amine]. It has been generally observed that distorted square-pyramidal coordination geometries dominate when one pyridine arm of tpa is replaced by a thioether group[24] or oxygen donor ligands such as carboxylate[19] or phenolate.[25−27] In contrast, copper complexes of tris(picolyl)amine (tpa) itself are always trigonal-bipyramidal.[28−31] The amino acid side chain functionalities in **1** and **2** did not affect the structural properties of our complexes. The benzyl substituent, unlike that in the corresponding trigonal-bipyramidal zinc complexes,[17] is flexible and does not interact with the copper(II) center. This is indicated by the X-ray structure analyses of **4a** and **8b**. The distance between copper(II) and the center of the phenyl ring is always larger than 7 Å, whereas it is only 4.5 Å in $[(\mathbf{2})(H_2O)Zn]^{2+}$.

The circular dichroism spectra of **4a**, **4b**, and **6** supported these observations, no indication of a structural change affecting the chiral amino acid moiety in **2** upon copper complexation being found. This is evident on comparison with the spectra of the free ligand and its trigonal-bipyramidal zinc(II) complexes. However, there were unique features in the spectra of **8a** and **8b** that cannot yet be explained. EPR and UV/Vis spectra, as well as the cyclic voltammograms of the compounds, further confirmed that the first coor-

dination sphere was not affected by the benzyl substituent in ligand **2**. Only the monodentate coligand induced measurable changes. It is interesting to note that we did not observe an effect of the benzyl substituent on electrode processes in the electrochemical measurements. Such phenomena have been discussed with regard to a series of cobalt(III) complexes containing nitrilotriacetic acid ligands derived from different amino acids including phenylalanine.[32]

Conclusions

Our results have demonstrated that the coordination geometry of complexes with amino acid derived ligands is a crucial determinant for the occurrence of weak noncovalent interactions. The benzyl substituent in the chiral ligand **2** is closely associated with zinc(II) in trigonal-bipyramidal complexes, but does not interact at all with the copper(II) center in square-pyramidal or octahedral coordination environments. This is an important consideration for the development of synthetic chiral metal complexes intended to exhibit metalloenzyme-like properties such as the activation or recognition of substrates by interactions involving the second, noncoordinating ligand sphere.

Experimental Section

General Methods: Spectra were recorded with the following instruments: UV/Vis spectra: Varian Cary 1G spectrophotometer. Cyclic voltammetry: PAR potentiostat 263 equipped with a three-electrode cell containing a glassy carbon working electrode, an Ag/AgCl reference electrode, and a Pt counterelectrode. Methanol solutions (10^{-3} M) of the complexes containing tetrabutylammonium hexafluorophosphate (TBAH, 0.1 M) as supporting electrolyte were used. Solutions were deoxygenated by bubbling with dry nitrogen. The reported potentials have not been corrected for junction potential effects. Under the measurement conditions, the ferrocene/ferrocenium couple was observed at +0.40 V. EPR spectra: Bruker ESP 300 E spectrometer. All spectra were recorded at 120 K in frozen methanol solutions at 10^{-3} M copper concentrations. Circular dichroism: Jasco J710 Spectropolarimeter. IR: Mattson Polaris FTIR. All complexes were prepared and stored under dry nitrogen. The workup was performed under ambient laboratory conditions unless stated otherwise. Absolute solvents were purchased from Fluka and stored under nitrogen. Solvents were used without further purification. All other reagents were of commercially available reagent-grade quality. The syntheses of the ligands bpaAc-Gly-OEt (**1**) and bpaAc-Phe-OMe (**2**),[17] and of the copper complexes [(bpaAc-Gly-OEt)CuCl](OTf) (**7a**) and [(bpaAc-Gly-OEt)-$CuCl]_2[CuCl_3(MeOH)]Cl$ (**7b**)[18] are described elsewhere.

General Synthetic Procedure: The complexes **3a**, **3b**, **4a**, **4b**, and **5** were prepared by the same procedure described below. However, the subsequent workup and purification were slightly different for each compound and are therefore described separately. Solid Cu^{2+} salt was added in one portion to a stirred solution of 1 equiv. of the respective ligand in MeCN. In the case of [(bpaAc-Gly-OEt)(*N*-Meim)Cu]$(OTf)_2$ (**5**), *N*-methylimidazole was added after 15 min. Stirring was continued overnight at room temperature, followed by removal of all solvent in a vacuum.

[(bpaAc-Gly-OEt)(H_2O)Cu(ClO_4)](ClO_4)·H_2O (3a): This compound was prepared from **1** (243 mg, 0.71 mmol) and $Cu(ClO_4)_2$·$6H_2O$ (263 mg, 0.71 mmol) in MeCN (5 mL). The solid residue was suspended in a minimum of MeOH, and the resulting blue precipitate was separated from the green filtrate, dried in a vacuum, and completely dissolved in hot MeOH. The solution was left at 4 °C for several days, yielding **3a** as a blue solid that was isolated and dried in a vacuum. Single crystals suitable for an X-ray structure analysis where obtained by slow recrystallization from MeOH at 4 °C over a period of several weeks. Yield: 296 mg (0.46 mmol, 65%). $C_{18}H_{24}Cl_2CuN_4O_{12}$·$H_2O$ (640.9): calcd. C 33.74, H 4.09, N 8.74; found C 33.97, H 4.14, N 8.72. FAB-MS (nitrobenzyl alcohol): *m*/*z* = 504 [(bpaAc-Gly-OEt)Cu(ClO_4)]$^+$, 405 [(bpaAc-Gly-OEt)Cu]$^+$. IR (KBr): $\tilde{\nu}$ = 1723 cm^{-1} (COOEt), 1658 (amide I), 1105 (ClO_4). UV/Vis (MeOH): λ_{max} (lg ε) = 706 nm (1.88).

[(bpaAc-Gly-OEt)(H_2O)Cu(OTf)](OTf)·0.3CH_2Cl_2 (3b): This compound was prepared from **1** (483 mg, 1.41 mmol) and $Cu(OTf)_2$ (510 mg, 1.41 mmol) in MeCN (15 mL). The crude product was treated with CH_2Cl_2 (10 mL) and the mixture was cooled to −20 °C and filtered to remove insoluble impurities. The volume of the filtrate was reduced, and some diethyl ether was added. Storage of the solution at −20 °C and repeated addition of Et_2O afforded the product as blue needles, which were isolated by filtration and dried in a vacuum. Recrystallization from CH_2Cl_2 by slow evaporation of the solvent under dry nitrogen afforded blue crystals suitable for X-ray structure analysis. Yield: 593 mg (0.79 mmol, 56%). $C_{20}H_{24}CuF_6N_4O_{10}S_2$·0.3$CH_2Cl_2$ (747.6): calcd. C 32.62, H 3.32, N 7.49; found C 32.45, H 3.34, N 7.40. FAB-MS (nitrobenzyl alcohol): *m*/*z* = 554 [(bpaAc-Gly-OEt)Cu(OTf)]$^+$, 405 [(bpaAc-Gly-OEt)Cu]$^+$. IR (KBr): $\tilde{\nu}$ = 1749 cm^{-1} (COOEt), 1663 (amide I), 1287, 1254, 1171, 1032 (OTf). UV/Vis (MeOH): λ_{max} (lg ε) = 706 nm (1.85).

[(bpaAc-Phe-OMe)(MeCN)Cu](ClO_4)$_2$·H_2O (4a): This compound was prepared from **2** (508 mg, 1.21 mmol) and $Cu(ClO_4)_2$·$6H_2O$ (448 mg, 1.21 mmol) in MeCN (10 mL). CH_2Cl_2 (5 mL) was added to the crude product, and the resulting suspension was decanted. The residue was dried in a vacuum and dissolved in 10 mL of MeCN. Slow diffusion of Et_2O into this solution afforded the product as blue needles, which were isolated and dried in a vacuum. Some of these crystals were suitable for X-ray structure analysis. Yield: 772 mg (1.07 mmol, 88%). $C_{26}H_{31}Cl_2CuN_5O_{12}$ (740.0): calcd. C 42.20, H 4.22, N 9.46; found C 42.31, H 4.38, N 9.40. FAB-MS (nitrobenzyl alcohol): *m*/*z* = 580 [(bpaAc-Phe-OMe)Cu(ClO_4)]$^+$, 481 [(bpaAc-Phe-OMe)Cu]$^+$. IR (KBr): $\tilde{\nu}$ = 1749 cm^{-1} (COOEt), 1659 (amide I), 1103 (ClO_4). UV/Vis (MeOH): λ_{max} (lg ε) = 709 nm (1.85). CD (10^{-3} M in methanol): λ [nm] ([θ]/1000 [°cm^2dmol^{-1}]) = 219 (+28.2), 263 (−1.5), 282 (+1.6).

[(bpaAc-Phe-OMe)(H_2O)Cu](OTf)$_2$ (4b): This compound was prepared from bpaAc-Phe-OMe (713 mg, 1.70 mmol) and $Cu(OTf)_2$ (615 mg, 1.70 mmol) in MeCN (20 mL). The crude product was dissolved in 5 mL of CH_2Cl_2 and filtered. Cooling of the filtrate overnight at −20 °C yielded the complex as a blue precipitate. The suspension was decanted and the residue was dried in a vacuum. Yield: 1.133 g (1.42 mmol, 84%). $C_{26}H_{28}CuF_6N_4O_{10}S_2$ (798.2): calcd. C 39.12, H 3.54, N 7.02; found C 39.27, H 3.66, N 6.87. FAB-MS (nitrobenzyl alcohol): *m*/*z* = 630 [(bpaAc-Phe-OMe)Cu(OTf)]$^+$, 481 [(bpaAc-Phe-OMe)Cu]$^+$. IR (KBr): $\tilde{\nu}$ = 1746 (COOMe), 1657 (amide I), 1282, 1253, 1166, 1031 (OTf). UV/Vis (MeOH): λ_{max} (lg ε) = 713 nm (1.83). CD (10^{-3} M in methanol): λ [nm] ([θ]/1000 [°cm^2dmol^{-1}]) = 217 (+25.4), 262 (−2.2), 282 (+1.0).

[(bpaAc-Gly-OEt)(*N*-Meim)Cu](OTf)$_2$ (5): This compound was prepared from **1** (382 mg, 1.11 mmol), Cu(OTf)$_2$ (402 mg, 1.11 mmol), and *N*-Meim (91 mg, 1.11 mmol) in MeCN (5 mL). The residual solid was dissolved in 5 mL of CH_2Cl_2, cooled to −20 °C and filtered to yield a clear blue solution. After reduction of the filtrate, diethyl ether was added. The mixture was stored at −20 °C to precipitate the product, which was isolated by filtration and dried in a vacuum. X-ray quality crystals were grown by layering a solution of **5** in a minimum of CH_2Cl_2 with diethyl ether for several days at 4 °C. Yield: 703 mg (0.89 mmol, 80%). $C_{24}H_{28}CuF_6N_6O_9S_2$ (786.2): calcd. C 36.67, H 3.59, N 10.69; found C 36.73, H 3.78, N 10.60. FAB-MS (nitrobenzyl alcohol): *m/z* = 554 [(bpaAc-Gly-OEt)Cu(OTf)]$^+$, 405 [(bpaAc-Gly-OEt)Cu]$^+$. IR (KBr): $\tilde{\nu}$ = 1732 cm^{-1} (COOEt), 1666 (amide I), 1282, 1247, 1157, 1031 (OTf). UV/Vis (MeOH): λ_{max} (lg ε) = 675 nm (1.93).

[(bpaAc-Phe-OMe)(*N*-Meim)Cu](OTf)$_2$ (6): *N*-Methylimidazole (18 μL, 0.23 mmol) was added in one portion to a stirred solution of **4b** (187 mg, 0.23 mmol) in 10 mL of MeCN. Stirring was continued overnight at room temperature, followed by removal of all solvent in a vacuum. The resulting solid was dissolved in 5 mL of CH_2Cl_2 and stored at −20 °C overnight. After filtration, diethyl ether was added dropwise to cause a slight cloudiness. The mixture was stored again at −20 °C to afford a blue precipitate, which was isolated by decantation of the supernatant and dried in a vacuum. In order to maximize yields it was necessary to isolate the product quickly, because it redissolved at room temperature. Yield: 177 mg (0.20 mmol, 87%). $C_{30}H_{32}CuF_6N_6O_9S_2$ (862.3): calcd. C 41.79, H 3.74, N 9.75; found C 41.73, H 3.81, N 9.50. FAB-MS (nitrobenzyl alcohol): *m/z* = 630 [(bpaAc-Phe-OMe)Cu(OTf)]$^+$, 481 [(bpaAc-Phe-OMe)Cu]$^+$. IR (KBr): $\tilde{\nu}$ = 1744 (COOMe), 1661 (amide I), 1282, 1255, 1162, 1031 (OTf). UV/Vis (MeOH): λ_{max} (lg ε) = 681 nm (1.91). CD (10^{-3} M in methanol): λ [nm] ([θ]/1000 [°cm^{2}dmol^{-1}]) = 218 (+27.6), 282 (1.3).

[(bpaAc-Phe-OMe)CuCl]$_2$[CuCl$_4$]·MeOH (8b) and [(bpaAc-Phe-OMe)CuCl](OTf) (8a): Solid $CuCl_2 \cdot 2H_2O$ (189 mg, 1.11 mmol) was added in one portion to a stirred solution of **2** (309 mg, 0.74 mmol) in 20 mL of MeOH. Stirring was continued overnight at room temperature. The volume of the solution was reduced, and storage at −20 °C afforded the product as a green solid. The complex was redissolved in the minimum possible amount of MeOH and recrystallized by slow diffusion of Et_2O into the solution. Diamond-shaped, green crystals were obtained. C,H,N, elemental analysis indicated the formulation [(bpaAc-Phe-OMe)CuCl]$_2$[CuCl$_4$]·MeOH for this compound. Single crystals suitable for X-ray structure analysis were obtained by slow recrystallization from MeOH at −20 °C. It was necessary to isolate the crystals quickly, because they rapidly redissolved at room temperature. The X-ray structure analysis indicates that the single crystals contained 3 molecules of MeOH per copper complex. For spectroscopic studies, the complex salt **8a** was generated in situ by addition of aqueous NaCl (2.5 or 1 M: 10% excess; saturated solution: large excess) to a solution of **4b** in methanol. The reaction was monitored by UV/Vis, EPR, or circular dichroism spectroscopy and run to completeness. Spectroscopic data are reported for both salts **8a** and **8b**. Yield (**8b**): 405 mg (0.31 mmol, 84%). $C_{48}H_{54}Cl_6CuN_8O_7 \cdot MeOH$ (1290.4): calcd. C 45.61, H 4.53, N 8.68; found C 45.46, H 4.46, N 8.74. FAB-MS (nitrobenzyl alcohol): *m/z* = 516 [(bpaAc-Phe-OMe)CuCl]$^+$, 481 [(bpaAc-Phe-OMe)Cu]$^+$. IR (KBr): $\tilde{\nu}$ = 1743 (COOMe), 1654 (amide I). UV/Vis (MeOH): **8a:** λ_{max} (lg ε) = 732 nm (1.96); **8b:** λ_{max} (lg ε) = 755 nm (2.30). CD (10^{-3} M in methanol): **8a:** λ [nm] ([θ]/1000 [°cm^{2}dmol^{-1}]) = 216 (21.4), 289 (2.3); **8b:** λ [nm] ([θ]/1000 [°cm^{2}dmol^{-1}]) = 221 (27.6), 288 (5.3).

X-ray Data Collection and Structure Refinement Details: Crystal data and experimental conditions are listed in Table 1. The molecular structures are illustrated in Figures 1−5. Selected bond lengths and bond angles, with standard deviations in parentheses, are summarized in Table 2. Intensity data were collected with graphite-monochromated Mo-K_α radiation with a Nonius CAD MACH3 diffractometer (**3a**, **5**), with a Nonius Kappa CCD area detector (**4a**, **8b**), and with a Siemens SMART 5000 CCD-diffractometer (exposure time: 10 s/frame, Δω = 0.3°, **3b**). The collected reflections were corrected for Lorentz, polarization, and absorption effects.[33] All structures were solved by direct methods and refined by full-matrix, least-squares methods on F^2.[34−36] Non-hydrogen atoms were refined with anisotropic thermal parameters. Hydrogen atoms were calculated for idealized geometries and allowed to ride on their parent atoms with isotropic displacement parameters related to those of the adjacent atoms by a factor of 1.5. CCDC-172745 (**3a**), -173039 (**3b**), -173635 (**4a**), -172744 (**5**), and -173634 (**7b**) contain the supplementary crystallographic data for this paper. These data can be obtained free of charge at www.ccdc.cam.ac.uk/conts/retrieving.html or from the Cambridge Crystallographic Data Centre, 12, Union Road, Cambridge CB2 1EZ, UK 8Fax: (internat.) + 44-1223/336-033; E-mail: deposit@ccdc.cam.ac.uk].

Acknowledgments

The authors gratefully acknowledge financial support from the Deutsche Forschungsgemeinschaft. We also thank Professor Rudi van Eldik for his generous support.

[1] C. A. Hunter, J. K. M. Sanders, *J. Am. Chem. Soc.* **1990**, *112*, 5525−5534.
[2] C. A. Hunter, *Angew. Chem.* **1993**, *105*, 1653−1655; *Angew. Chem. Int. Ed. Engl.* **1993**, *32*, 1584−1586.
[3] K. M. Guckian, B. A. Schweitzer, R. X. F. Ren, C. J. Sheils, P. L. Paris, D. C. Tahmassebi, E. T. Kool, *J. Am. Chem. Soc.* **1996**, *118*, 8182−8183.
[4] C. Chipot, R. Jaffe, B. Maigret, D. A. Pearlman, P. A. Kollmann, *J. Am. Chem. Soc.* **1996**, *118*, 11217−11224.
[5] K. M. Guckian, B. A. Schweitzer, R. X.-F. Ren, C. J. Sheils, D. C. Tahmassebi, E. T. Kool, *J. Am. Chem. Soc.* **2000**, *122*, 2213−2222.
[6] S. D. Zaric, D. M. Popovic, E. W. Knapp, *Chem. Eur. J.* **2000**, *6*, 3935−3942.
[7] C. Janiak, *J. Chem. Soc., Dalton Trans.* **2000**, 3385−3396.
[8] S. Mecozzi, A. P. West, D. A. Dougherty, *J. Am. Chem. Soc.* **1996**, *118*, 2307−2308.
[9] J. C. Ma, D. A. Dougherty, *Chem. Rev.* **1997**, *97*, 1303−1324.
[10] J. P. Klinman, *Chem. Rev.* **1996**, *96*, 2541−2561.
[11] O. Yamauchi, *Pure Appl. Chem.* **1995**, *67*, 297−304.
[12] P. Hu, C. Sorensen, M. L. Gross, *J. Am. Soc. Mass Spectrom.* **1995**, *6*, 1079−1085.
[13] G. Maccarrone, G. Nardin, L. Randaccio, G. Tabbi, M. Rosi, A. Sgamellotti, E. Rizzarelli, E. Zangrando, *J. Chem. Soc., Dalton Trans.* **1996**, 3449−3453.
[14] L. H. Abdel-Rahman, L. Battaglia, M. R. Mahmoud, *Polyhedron* **1996**, *15*, 327−334.
[15] T. Sugimori, H. Masuda, N. Ohata, K. Koiwai, A. Odani, O. Yamauchi, *Inorg. Chem.* **1997**, *36*, 576−583.
[16] Y. Shimazaki, H. Yokoyama, O. Yamauchi, *Angew. Chem.* **1999**, *111*, 2561−2562; *Angew. Chem. Int. Ed.* **1999**, *38*, 2401−2403.
[17] N. Niklas, O. Walter, R. Alsfasser, *Eur. J. Inorg. Chem.* **2000**, 1723−1731.
[18] N. Niklas, S. Wolf, G. Liehr, C. E. Anson, A. K. Powell, R. Alsfasser, *Inorg. Chim. Acta* **2001**, *314*, 126−132.
[19] T. Okuno, S. Ohba, Y. Nishida, *Polyhedron* **1997**, *16*, 3765−3774.

[20] T. Kobayashi, T. Okuno, T. Suzuki, M. Kunita, S. Ohba, Y. Nishida, *Polyhedron* **1998**, *17*, 1553−1559.
[21] J. W. Canary, C. S. Allen, J. M. Castagnetto, Y.-H. Chiu, P. J. Toscano, Y. Wang, *Inorg. Chem.* **1998**, *37*, 6255−6262.
[22] N. Niklas, unpublished results.
[23] C. W. Lee, F. C. Anson, *Inorg. Chem.* **1984**, *23*, 837−844.
[24] Y. Nishida, K. Takahashi, *Inorg. Chem.* **1988**, *27*, 1406−1410.
[25] R. Uma, R. Viswanathan, M. Palaniandavar, M. Lakshminarayanan, *J. Chem. Soc., Dalton Trans.* **1994**, 1219−1226.
[26] H. Adams, N. A. Bailey, I. K. Campbell, D. E. Fenton, Q. Y. He, *J. Chem. Soc., Dalton Trans.* **1996**, 2233−2237.
[27] S. Ito, S. Nishino, H. Itoh, S. Ohba, Y. Nishida, *Polyhedron* **1998**, *17*, 1637−1642.
[28] K. D. Karlin, J. C. Hayes, S. Juen, J. P. Hutchinson, J. Zubieta, *Inorg. Chem.* **1982**, *21*, 4106−4108.
[29] H. Nagao, N. Komeda, M. Mukaida, M. Suzuki, K. Tanaka, *Inorg. Chem.* **1996**, *35*, 6809−6815.
[30] H. Zheng, L. Que, Jr., *Inorg. Chim. Acta* **1997**, *263*, 301−307.
[31] B. S. Lim, R. H. Holm, *Inorg. Chem.* **1998**, *37*, 4898−4908.
[32] H. Kumita, K. Jitsukawa, H. Masuda, H. Einaga, *Inorg. Chim. Acta* **1998**, *283*, 160−166.
[33] [33a] A. C. T. North, D. C. Phillips, F. S. Mathews, *Acta Crystallogr., Sect. A* **1968**, *24*, 351−359. [33b] *COLLECT*, data collection software, B. V. Nonius, **1998**. [33c] *SCALEPACK*, data processing software: Z. Otwinowski, W. Minor, *Methods Enzymol.* **1997**, *276*, 307 (Macromolecular Crystallography, Part A).
[34] A. Altomare, G. Cascarano, C. Giacovazzo, A. Guagliardi, *J. Appl. Crystallogr.* **1993**, *26*, 343−350.
[35] G. M. Sheldrick, *SHELXTL-PC*, Siemens Analytical X-ray Instruments, Inc., Madison, WI, USA, **1994**.
[36] G. M. Sheldrick, *SHELXL-97*, Universität Göttingen, **1997**.

Received November 9, 2001
[I01447]